2018

Evaluating Soil Moisture–Precipitation Interactions Using Remote Sensing: A Sensitivity Analysis

Trent W. Ford
Southern Illinois University, twford@siu.edu

Steven M. Quiring
Ohio State University, quiring.10@osu.edu

Balbhadra Thakur
Southern Illinois University

Rohit Jogineedi
Southern Illinois University

Adam Houston
University of Nebraska—Lincoln, ahouston2@unl.edu

See next page for additional authors

Evaluating Soil Moisture–Precipitation Interactions Using Remote Sensing: A Sensitivity Analysis

TRENT W. FORD,[a] STEVEN M. QUIRING,[b] BALBHADRA THAKUR,[c] ROHIT JOGINEEDI,[d] ADAM HOUSTON,[e] SHANSHUI YUAN,[b] AJAY KALRA,[c] AND NOAH LOCK[f]

[a] *Department of Geography and Environmental Resources, Southern Illinois University, Carbondale, Illinois*
[b] *Department of Geography, Ohio State University, Columbus, Ohio*
[c] *Department of Civil and Environmental Engineering, Southern Illinois University, Carbondale, Illinois*
[d] *Department of Mechanical Engineering, Southern Illinois University, Carbondale, Illinois*
[e] *Department of Earth and Atmospheric Sciences, University of Nebraska–Lincoln, Lincoln, Nebraska*
[f] *Weather Decision Technologies, Norman, Oklahoma*

(Manuscript received 19 December 2017, in final form 21 June 2018)

ABSTRACT

The complex interactions between soil moisture and precipitation are difficult to observe, and consequently there is a lack of consensus as to the sign, strength, and location of these interactions. Inconsistency between soil moisture–precipitation interaction studies can be attributed to a multitude of factors, including the difficulty of demonstrating causal relationships, dataset differences, and precipitation autocorrelation. The purpose of this study is to explore these potential confounding factors and determine which are most important for consideration when assessing statistical coupling between soil moisture and precipitation. Soil moisture is assessed via three remote sensing datasets: the Advanced Microwave Scanning Radiometer for Earth Observing System, the Tropical Rainfall Measuring Mission Microwave Imager, and the Essential Climate Variable Soil Moisture. Estimates of soil moisture are coupled with afternoon thunderstorm events identified by the Thunderstorm Observation by Radar (ThOR) algorithm, and dry soil or wet soil preferences for convection initiation are determined for over 16 000 thunderstorm events between 2005 and 2007. Differences in soil moisture datasets were found to have the largest impact with regard to determining wet or dry soil preferences. Precipitation autocorrelation is prevalent in the data; however, precipitation autocorrelation did not influence the results with regard to dry or wet soil preferences. Consideration of the convective environment (i.e., weakly or synoptically forced) did result in significant differences in wet/dry soil preference, but only for certain soil moisture datasets. The results suggest that observation-driven soil moisture–precipitation interaction studies should both consider the convective environment and implement multiple soil moisture datasets to assure robust results.

1. Introduction

Soil moisture is an important component of water balance, and it is a key parameter that influences land–atmosphere interactions by modifying energy and water fluxes in the boundary layer (Eltahir 1998; Legates et al. 2011). Soil moisture plays an integrative role because it directly influences atmospheric, geomorphic, hydrologic, and biologic processes (Legates et al. 2011).

Soil moisture is a key variable for land–atmosphere interactions because it governs evapotranspiration and the partitioning of the surface–atmosphere energy flux (McPherson 2007; Alfieri et al. 2008). It is through modifications in evapotranspiration that soil moisture can potentially affect precipitation and near-surface temperature (Findell et al. 2011; Miralles et al. 2012; Hu et al. 2017). Soil moisture feedbacks that can influence precipitation on convective time scales (i.e., diurnal) can generally be divided into wet soil and dry soil processes. When soil moisture is abundant (i.e., wet soil), this can increase evapotranspiration and latent heat exchange with the atmosphere. These processes tend to lower the lifting condensation level (LCL) and level of free convection (LFC), and increase convective energy. The increase in convective available potential energy (CAPE) and the lower LCL and LFC tend to trigger deep convection and can lead to rainfall (Pal and Eltahir 2001; Santanello et al. 2011). On the other hand, dry soils increase sensible heat and the Bowen ratio, elevating the LCL and LFC. While these dry soil processes can inhibit

Corresponding author: Trent W. Ford, twford@siu.edu

DOI: 10.1175/JHM-D-17-0243.1

deep convection if parcels are unable to reach the LCL, strong sensible heating can help erode convective inhibition and thereby lead to convection initiation and precipitation (Taylor et al. 2011; Ford et al. 2015a). General circulation models have shown a preference in most regions of the world for positive (i.e., wet soil) soil moisture feedbacks to precipitation (Koster et al. 2004; Taylor et al. 2012). In contrast, observation-based studies on regional to global scales have found evidence for both positive (wet soil) and negative (dry soil) feedbacks (Findell and Eltahir 2003; Taylor et al. 2011; Ferguson and Wood 2011; Ford et al. 2015a).

The lack of consensus on the sign and strength of soil moisture–precipitation coupling is attributed to a multitude of confounding factors, including the difficulty of establishing causality when using observations (e.g., Tuttle and Salvucci 2017). Specifically, issues such as how to account for atmospheric persistence/precipitation persistence (Taylor et al. 2011) and how to account for time-scale variability (Tuttle and Salvucci 2017) have been shown to have a significant impact on the results of statistically based studies of soil moisture–precipitation feedbacks. These issues can potentially result in uncertainty regarding the sign and strength of the soil moisture–precipitation feedbacks. Precipitation persistence refers to precipitation that is highly clustered on daily time scales, but not due to a soil moisture feedback. Given this situation, precipitation that occurs on a day following a precipitation day may falsely indicate a positive soil moisture feedback, when in reality both precipitation events were caused by the same large-scale weather system. Precipitation persistence can artificially inflate the strength of a positive or negative (i.e., Wei et al. 2008) soil moisture feedback. This issue is difficult to account for when using observational data to quantify soil moisture–precipitation feedbacks, and it requires using more sophisticated statistical methods than Pearson product-moment correlation (e.g., Taylor et al. 2012; Guillod et al. 2015; Tuttle and Salvucci 2016). The second issue that can confound observation-based analyses of soil moisture–precipitation feedbacks, as detailed by Tuttle and Salvucci (2017), is time-scale variability. That is, correlations between daily soil moisture and precipitation, computed on seasonal-to-interannual time scales, can be confounded by the close relationship between soil moisture and precipitation on these longer time scales. For example, growing seasons that exhibit wetter-than-normal soils will also experience abundant precipitation, and these types of relationships can inflate correlations between soil moisture and precipitation on daily time scales. This issue can be more easily overcome by time filtering, for example, removing mean seasonal or annual cycles (Tuttle and Salvucci 2017).

In addition to these two issues raised by Tuttle and Salvucci (2017), we have identified two additional factors that warrant consideration when using observations to quantify soil moisture–precipitation coupling at daily time scales: dataset dependency and convection initiation versus precipitation. The first of these issues, dataset dependency, refers to the degree to which soil moisture feedback signals are dependent on the soil moisture or precipitation dataset used. In this study, we will focus on soil moisture dataset dependency, because our analysis does not rely on precipitation observations (see below). Many studies infer soil moisture–precipitation feedback from a single source of soil moisture information, whether in situ measurement, remote sensing observation, or model simulation. Many studies have evaluated the differences between these soil moisture datasets (e.g., Albergel et al. 2012; Su et al. 2013; Tuttle and Salvucci 2014; Dirmeyer et al. 2016), but there is a dearth of studies examining the influence of dataset dependency on the consistency of soil moisture–precipitation feedback sign and strength. This is particularly important for microwave remote sensing soil moisture datasets, as their utility for land–atmosphere interaction investigation has grown exponentially in the last decade. The second issue that needs to be considered is the use of precipitation observations to infer soil moisture–precipitation coupling on convective time scales. Although precipitation is an important end product of soil moisture feedback, the mechanisms connecting soil moisture to atmospheric processes that lead to precipitation often occur upwind of where the precipitation actually falls. Therefore, evaluating the statistical relationship between soil moisture and precipitation using the soil moisture immediately underlying the point of precipitation may result in a spatial mismatch because the soil moisture conditions that actually feed back to the atmosphere may not be collocated with the point at which the precipitation occurred.

The purpose of this study is to examine how these confounding factors influence the sign and strength of soil moisture–precipitation coupling in the U.S. Great Plains. Here we define the Great Plains as the area between 30° and 50°N latitude and between 105° and 90°W longitude. Our primary objective is not to determine whether this region is dominated by a positive (wet soil) or negative (dry soil) feedback, but to document how these confounding factors influence land–atmosphere coupling studies. Our findings shall help inform observationally based studies of land–atmosphere interactions, especially those that rely on satellite-derived soil moisture, by identifying best practices.

TABLE 1. Microwave remote sensing soil moisture datasets.

Product	Version	Frequency	Spatial resolution	Spatial extent	Temporal extent
AMSR-E	LPRM_AMSRE_SOILM3.002	10.65 GHz (X band)	0.25°	Global	2003–10
TMI	LPRM_TMI_NT_SOILM3.001	10.65 GHz (X band)	0.25°	40°N–40°S, 180°–180°	1998–2015
ECV	SM v03.2 COMBINED	Varied	0.25°	Global	1979–present

2. Data

a. Soil moisture

We use microwave-based soil moisture retrievals from three different sources: the Advanced Microwave Scanning Radiometer for Earth Observing System (AMSR-E), the Tropical Rainfall Measuring Mission (TRMM) Microwave Imager (TMI), and the Essential Climate Variable Soil Moisture (ECV-SM) dataset (Table 1). Herein, these products will be identified as AMSR-E, TMI, and ECV. AMSR-E was developed by the joint venture of the U.S. National Aeronautics and Space Administration (NASA) and the Japan Aerospace Exploration Agency (JAXA), to fly on the *Aqua* platform, and was operational from 2002 until 2011. Soil moisture is estimated with AMSR-E based on inversion of the radiative transfer models that link Earth surface parameters with the observed AMSR-E brightness temperature (Njoku et al. 2003). Volumetric water content estimates as part of the Land Parameter Retrieval Model (LPRM)-based Level-3 surface soil moisture dataset (Owe et al. 2008) were used in this study. AMSR-E soil moisture has been used in numerous land–atmosphere interaction studies (Ferguson and Wood 2011; Taylor et al. 2011, 2012; Guillod et al. 2015) because of its global coverage and relatively long period of record. The descending AMSR-E retrievals were used in this study to capture morning soil moisture conditions prior to afternoon convection.

TMI is a dual-polarized passive radiometer that was launched in 1997 on the TRMM platform (Kummerow et al. 1998; Bindlish et al. 2003). Volumetric water content is estimated from the TMI land surface temperature observations using the Land Parameter Retrieval Model, and soil moisture is reported twice daily as part of the TMI product (Owe et al. 2008; Gao et al. 2006). The LPRM-based Level-3 nighttime surface soil moisture dataset was used in this study, as its retrieval time (variable, but 0130 LST on average) was closest to (but not coinciding with) the 1200–2000 LST afternoon convective time period. Although TMI has a finer spatial resolution than AMSR-E (Table 1), its spatial extent does not cover our entire study area; TMI soil moisture is not available north of 40°N latitude. Therefore, analysis of TMI soil moisture in this study is conserved to the study region south of 40°N latitude. Soil moisture from the TMI dataset has been previously used for land–atmosphere interaction investigations (Frye and Mote 2010), but, despite its longer time record and finer spatial resolution, it is less popular than AMSR-E for these types of studies.

The ECV dataset is a merged active and passive microwave remote sensing–based soil moisture dataset that is produced under the European Space Agency's Climate Change Initiative (Liu et al. 2012; Dorigo et al. 2015). ECV integrates soil moisture retrievals from SMMR, SSM/I, TMI, AMSR-E, Active Microwave Instrument (AMI), and ASCAT sensors, resulting in a global soil moisture product with a climatologically sufficient record length (from 1979 to present). It is important to note here that the ECV soil moisture dataset contains information from both AMSR-E and TMI; the former informed ECV estimates from 2002 to 2011, the latter from 1998 to 2002 (Dorigo et al. 2017). Previous land–atmosphere interaction studies have found great utility in the ECV soil moisture dataset (Guillod et al. 2014; Hirschi et al. 2014; Zhou et al. 2016). ECV is a daily product, but because it blends multiple datasets, we could not confirm all soil moisture sources informing the ECV product were observed prior to the afternoon thunderstorm events on the same day. Therefore, we use the ECV soil moisture from the previous day to account for this issue.

Prior to their use in this study, we validated each remote sensing soil moisture product against in situ observations from 83 stations in the Oklahoma Mesonet. These high-quality observations (see Scott et al. 2013) were used to determine if any of the three satellite datasets exhibited a consistent wet or dry soil bias, which would likely perpetuate to our soil moisture coupling results. Daily soil moisture values, expressed as standardized anomalies of volumetric water content from each dataset, were compared to observations from the Oklahoma Mesonet station that fell within the corresponding satellite grid cell; validation statistics were computed using daily data between May and September over a dataset-varying time period (AMSR-E, 2003–10; TMI, 2003–14; ECV, 2003–14). Anomaly biases for all three datasets are quite small, positive (wet bias) for AMSR-E and negative (dry bias) for TMI and ECV. However, mean absolute errors are much larger, exceeding half a standard deviation beyond the mean, suggesting that the bias is not systematic. Indeed,

correlations between the satellite–in situ soil moisture anomaly difference (i.e., residuals) and the actual in situ soil moisture anomaly are strongly negative for all three satellite products (Table 2). This indicates that all three products exhibit wet biases when the in situ anomaly is negative (i.e., dry) and dry biases when the in situ anomaly is positive (i.e., wet). This nonsystematic bias does tend to affect the ability of the satellite products to distinguish between wet and dry conditions, as compared with the in situ anomalies. Table 2 shows the wet and dry hit rates, which denote the number of concurrent satellite–in situ wet anomalies and dry anomalies, respectively, expressed as a percent of all in situ wet and dry anomalies. The wet hit rates are notably smaller than the dry hit rates, demonstrating that all three satellite datasets struggle to identify wetter than normal conditions. Despite the difference between wet and dry soil hit rates, the nonsystematic biases of all three products suggest that they will not consistently over- or underestimate soil moisture conditions and therefore can be compared with regard to the incidence and prevalence of wet and dry soil precipitation coupling.

TABLE 2. Soil moisture satellite remote sensing product validation using Oklahoma Mesonet (5 cm) in situ observations. Validation statistics are computed for both volumetric water content and standardized anomalies of volumetric water content. The residual correlation for the anomaly validation refers to the correlation coefficient between the satellite–in situ difference and the in situ observation. Correlations are calculated using all valid daily satellite–in situ soil moisture pairs. Wet and dry hit rates refer to the rate of concurrent wet or dry anomalies in the satellite and in situ soil moisture datasets, expressed as a percent of all wet or dry in situ anomalies.

Product	AMSR-E	TMI	ECV
Bias	0.011	−0.048	−0.026
Mean absolute error	0.734	0.791	0.750
R^2	0.266	0.222	0.294
Residual correlation	−0.785	−0.722	−0.765
Wet hit rate (%)	51.4	46.7	51.6
Dry hit rate (%)	88.0	86.8	88.3

b. *Convection initiation events*

Most investigations of soil moisture–precipitation feedback use changes in the probability, intensity, or total accumulation of convective (i.e., nonstratiform) precipitation as the atmospheric response to collocated soil moisture measurements. However, the dynamic and thermodynamic mechanisms coupling the terrestrial and atmospheric segments of the feedback process occur prior to the initiation of precipitation, and therefore the location of precipitation initiation or maximum precipitation accumulation are not necessarily the same as the location of convection initiation. Given this shortcoming, we argue that evaluating soil moisture underlying the location of convection initiation is more appropriate and provides a more robust physical connection with and insights to the associated physical processes. To identify convection initiation across the United States Great Plains, we use the Thunderstorm Observation by Radar (ThOR; Houston et al. 2015) algorithm. ThOR fuses multisensor datasets, including Level-II radar from the network of Weather Surveillance Radar-1988 Doppler (WSR-88D) sites, lightning data from the National Lightning Detection Network, and storm motion estimates from the North American Regional Reanalysis. This multisource provides a more robust characterization of thunderstorms, defined as deep moist convection producing thunder (i.e., Houston et al. 2015), than single-source approaches. ThOR is capable of cataloging nearly every thunderstorm event that occurs over regional-scale to continental-scale domains. Nonconvective precipitation is not included in this analysis as ThOR filters out stratiform precipitation prior to thunderstorm identification (Houston et al. 2015). Additionally, ThOR will not detect shallow convection, to the extent that shallow convection fails to produce column-maximum radar reflectivity exceeding 30 dBZ over an area greater than 50 km^2 and cloud-to-ground lightning. To focus analysis on the first initiation within an area, Lock and Houston (2014) used a 100-km threshold distance such that initiation points identified within 100 km of an established storm were considered connected to the ongoing convection and were not considered as an independent storm. This constraint was applied to the initiation points identified for this study.

Houston et al. (2015) verified ThOR against 166 manually analyzed deep convection tracks. The probability of ThOR detection compared to manual tracks was 0.889 and the false alarm rate was 0.108, suggesting robust performance for thunderstorm track detection (Houston et al. 2015). Beyond tracking errors, it is anticipated that the primary source of error in ThOR is its reliance on cloud-to-ground lightning and not on total lightning, as existing total lightning observations are too limited to serve as a basis for a robust continental United States (CONUS)-scale climatology. It is estimated that the exclusion of in-cloud lightning results in an approximately 25% underestimation of thunderstorm counts (Houston et al. 2015). Given the difficulty of manual thunderstorm identification and classification methods (e.g., Ford et al. 2015b), the propensity of the ThOR algorithm for large-scale implementation combined with the method's low error justifies its use here. ThOR provides a useful means of assessing soil moisture–precipitation feedback in the U.S. Great Plains without having to assume that precipitation is collocated with convection initiation.

Unfortunately, the ThOR algorithm is computationally intensive. Therefore, this study is based on thunderstorms during 2005, 2006, and 2007 that have been identified using ThOR. Because we focus our analysis on thunderstorm initiation and not precipitation initiation or total precipitation, we cannot estimate the percent of Great Plains warm season precipitation accounted for in this study. However, the 42 469 thunderstorm initiation points identified by ThOR between May and September in 2005–07 represents the vast majority of thunderstorms that initiated in the study region over this time period. Therefore, we can conclude with confidence that the 16 083 afternoon thunderstorm events analyzed in this study represent a large fraction of all warm season thunderstorms initiating in the Great Plains between 2005 and 2007. When we subset these afternoon thunderstorms by convective environment, events that initiated in a weakly forced environment represented between 12% and 15% of all 42 469 thunderstorms, depending on the method used for environment classification.

3. Methods

a. Soil moisture

Daily soil water content estimates from each of the three remote sensing datasets were converted to anomalies by subtracting the climatological (i.e., multiyear) mean of a 15-day moving window centered on that calendar day and dividing by the multiyear standard deviation in that same moving window. Although thunderstorm events are only available from 2005 to 2007, the AMSR-E, TMI, and ECV soil moisture anomalies were computed using daily soil moisture estimates over the time periods 2003–10, 1998–2014, and 1998–2014, respectively. This was done to ensure that the anomalies were calculated using a sufficiently long time series to produce stable values. The 15-day moving window was used to characterize relative soil wetness with respect to the soil moisture seasonal cycle that is exhibited in the Great Plains (e.g., Illston et al. 2008; Khong et al. 2015). This approach puts the soil moisture values into an appropriate context (with respect to the normal soil moisture values at that location and time of year). Percentiles of soil water content are frequently used to characterize the relative wetness of the soil (Taylor et al. 2011; Ford et al. 2016); however, using percentiles requires a sufficiently long data record and sufficient measurement precision such that each observation represents a unique percentile of the overall distribution. AMSR-E and TMI both report soil moisture estimates as a percentage of volumetric water content at 1% increments. This means if volumetric water content naturally varies between 10% and 40% (i.e., between 0.10 and 0.40 $cm^3 cm^{-3}$), there will only be 31 unique observations spread among 100 percentile values. This issue is demonstrated by showing the cumulative and probability distribution functions of the soil water content from an AMSR-E grid cell in northeastern Oklahoma (Fig. 1). The distributions are composed of daily soil moisture from the 15-day moving window surrounding the calendar day of 2 August (2003–10). The empirical cumulative distribution function (Fig. 1a) shows that the volumetric water content value of 0.26 $cm^3 cm^{-3}$ represents a range from the 42nd to the 70th percentile of the distribution. Clearly, we are unable to properly separate wetter-than-normal from drier-than-normal soil moisture conditions when ''normal''—presumably the distribution median—represents the same moisture conditions as the 45th and 65th percentiles. Additionally, since soil moisture distributions are often non-Gaussian (Fig. 1b), this precludes estimating percentiles using the mean and standard deviation. Therefore, standardizing daily soil moisture by simply using the mean and standard deviation, as is done in this study, provides a better representation of relatively dry or wet soils.

b. Convection initiation event classification

For our purposes, we focus only on afternoon thunderstorms in the Great Plains that occur during the warm season, May–September. We included all of the thunderstorm events that were identified by ThOR if the time of initiation occurred between 1200 and 2000 LST and no other thunderstorm events initiated within 50 km of that event between 0600 and 1200 LST. This resulted in a total of 16 083 thunderstorm events across our study region (Fig. 2). Although we only have data from three warm seasons, the number of thunderstorm events provides a sufficiently large sample size for our analysis. Many of the ThOR-identified thunderstorm events were due to large-scale, synoptic forcing such as a passing cold front, dryline, or midlevel trough. Although land surface conditions may have some influence on these events, the dominant influence is the synoptic forcing. Therefore, we implement a number of methods to identify which events are weakly forced (i.e., the events that are of interest in this study) and which events are synoptically forced. This classification will be used to identify the events where soil moisture feedbacks may play a role in triggering convection initiation. Additionally, separating weakly forced events from synoptically forced events is useful for accounting for precipitation autocorrelation (i.e., precipitation persistence). Precipitation autocorrelation is caused by large-scale weather systems, such as a passing mesoscale convective complex or an extratropical cyclone migrating along a stationary front, that cause precipitation to occur on two or more consecutive days. Therefore, by

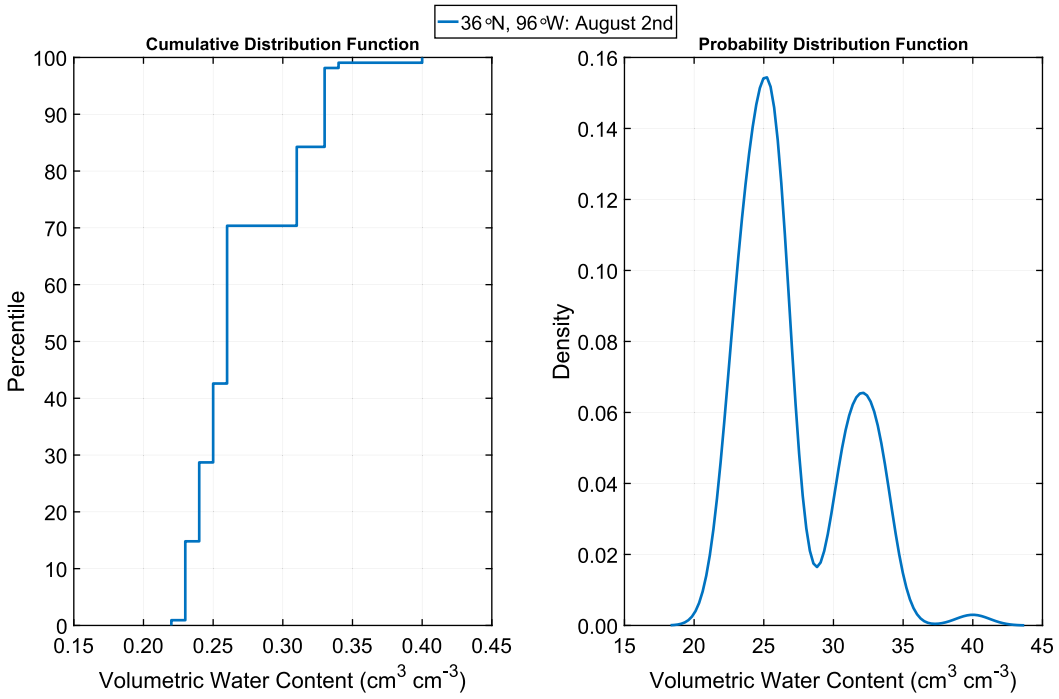

FIG. 1. (left) Cumulative distribution function and (right) probability distribution function of daily soil moisture within a 15-day moving window centered over the calendar day 2 Aug, including days from 2005, 2006, and 2007. Data are from an AMSR-E pixel over northeastern Oklahoma.

separating these types of events from convective triggering in weakly forced environments, we can isolate and remove precipitation persistence and maintain any daily precipitation autocorrelation that is due to soil moisture feedbacks.

An extensive literature search was undertaken to identify the best methods for determining the forcing environment of individual storm events, in an a posteriori investigation. However, there are a dearth of methods for classifying weakly forced and synoptically forced environments over large regions (i.e., thousands of kilometers) on climatological time scales. In this study, the Great Plains region is divided into twelve 5° × 5° areas (Table 3) in which all (raining and nonraining) days between 1 May 2005 and 30 September 2007 are classified as either weakly forced or synoptically forced. Any event occurring on a weakly forced day, for example, is classified similarly. Convective environments within each of the 12 areas are first classified through manual inspection of the daily (0600 LST) weather map produced by the National Oceanic and Atmospheric Administration's Weather Prediction Center (WPC) (http://www.wpc.ncep.noaa.gov/dailywxmap/). These maps are produced once daily and include the surface weather map and 500-hPa contours. Most importantly, the maps denote synoptic-scale features such as surface fronts and boundaries and midlevel troughs. Daily classification of the synoptic environment of each of the 12 subregions within the Great Plains was completed via visual inspection of the daily weather maps.

This procedure, herein referred to as manual classification, is adopted from multiple studies that consider an environment to be synoptically forced if a region is within close proximity to frontal boundaries, drylines, midlevel troughs, and closed surface lows and highs (Brown and Arnold 1998; Evans and Doswell 2001; Rose et al. 2008; French and Parker 2012). For our study, the distance between the edge of an area and the closest point on the edge of any of these synoptic features had to be no more than 200 km in order for that area's environment to be considered synoptically forced. We used the edge of these features instead of, for example, the center of a midlevel trough, as this made the visual reference easier. Brown and Arnold (1998) and Dixon and Mote (2003) implemented a similar, manual identification procedure only with a 500-km boundary for synoptic-scale features. Our decision to implement a tighter, 200-km boundary was made because 1) our boundary is implemented around an entire region instead of one city or one state and 2) using a 500-km boundary resulted in many days classified as "synoptically forced" as the synoptic feature was too far to affect the region within the

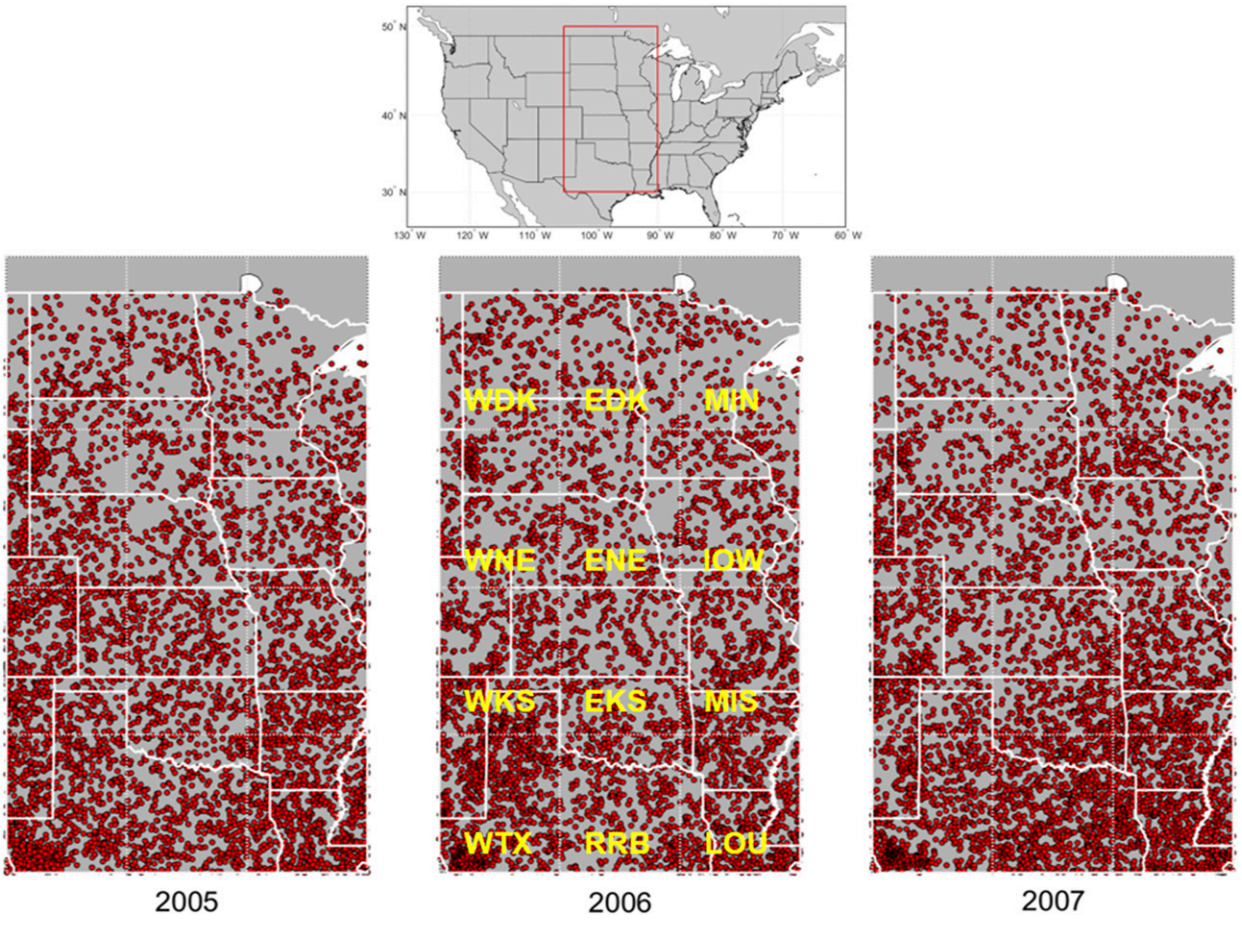

FIG. 2. Afternoon (1200–2000 LST) thunderstorm events identified using ThOR between 2005 and 2007.

24-h time period. Additionally, we experimented with 300- and 250-km boundaries, with no significant change in results. Daily weather maps were imported into ArcGIS and overlaid with subregion boundaries to determine if large-scale features affected each region during that day. The primary limitation of the daily weather maps are their temporal resolution, as they are most representative of surface and middle atmosphere conditions at 0600 LST in the Great Plains. This is less than ideal when characterizing the convective environment in which afternoon thunderstorms occur. To test the robustness of the maps for characterizing the afternoon convective environment, we randomly sampled 6 days per month over our study period (90 days total) and repeated the manual classification using 0000 UTC (1800 LST) surface weather maps produced by the WPC (http://www.wpc.ncep.noaa.gov/archives/web_pages/sfc/sfc_archive.php). Comparison of classification of each of the 90 days as either "synoptically forced" or "weakly forced" was undertaken for each region and is represented as a weak hit rate and a synoptic hit rate. These hit rates are computed as the number of matching weakly forced or synoptically forced classifications from both data sources, expressed as a percent of the total daily weather map weakly forced or synoptically forced classifications. Therefore, a weak hit rate of 80% means that 80% of all weakly forced classifications using the morning daily weather map were also weakly forced classifications in the evening surface weather map. Weak hit rates ranged from 78.5% in the Minnesota subregion to 100% in the West Kansas, West Nebraska, and West Dakota regions, with an overall study area average of 87.0%. Synoptic hit rates were slightly higher, ranging from 80% in the East Dakota subregion to 100% in the West Texas, West Nebraska, and East Kansas regions, and with an overall average of 90.5%. It should be noted here that the WPC surface weather maps do not include the location of midlevel atmospheric features such as midlevel troughs. This omission most likely results in an overestimation of weakly forced conditions in the WPC surface weather maps, as compared to the daily weather maps used in the manual classification. However, this limitation does not preclude a fair comparison between the WPC surface weather maps and the daily weather maps

TABLE 3. Regions of the Great Plains for which thunderstorm events were classified.

Region	Abbreviation	Spatial extent (lat, lon)	Afternoon thunderstorm events (2005–07)
West Texas	WTX	30°–35°N, 105°–100°W	2254
West Kansas	WKS	35°–40°N, 105°–100°W	1715
West Nebraska	WNE	40°–45°N, 105°–100°W	1367
West Dakotas	WDK	45°–50°N, 105°–100°W	670
Red River basin	RRB	30°–35°N, 100°–95°W	1672
East Kansas	EKS	35°–40°N, 100°–95°W	1225
East Nebraska	ENE	40°–45°N, 100°–95°W	982
East Dakotas	EDK	45°–50°N, 100°–95°W	680
Louisiana	LOU	30°–35°N, 95°–90°W	2401
Missouri	MIS	35°–40°N, 95°–90°W	1604
Iowa	IOW	40°–45°N, 95°–90°W	1039
Minnesota	MIN	45°–50°N, 95°–90°W	474

with regard to the robustness of the manual classification method. Despite the lack of information regarding midlevel atmospheric features in the WPC surface weather maps, the strong correspondence between the two products suggests that the manual classification—based on daily 0600 LST weather maps—is robust. Therefore, we expect the manual method sufficiently characterizes the afternoon convective environment, and, despite user error and subjectivity, the method is considered the "truth" to which the other, automated methods are compared. The results presented in this study are based on the manual classification method for discerning weakly and synoptically forced thunderstorm events.

Since our study only covers 3 years, it was feasible to employ manual classification; however, it would not be feasible to implement this approach globally or over longer time periods. Therefore, we also classified weakly and synoptically forced environments using three automated methods. The first automated method is adopted from Brown and Arnold (1998) and, more recently, Dixon and Mote (2003), and identifies weakly forced environments as those in which the area-averaged 500-hPa wind speed is less than 7.7 m s^{-1} and the area-averaged surface wind speed is less than 5.5 m s^{-1}. This method is herein known as the Georgia method, as it was implemented by Dixon and Mote (2003) for classifying convective environments that they related to the urban heat island effect in Atlanta, Georgia. The second automated method is adopted from Carleton et al. (2008a,b) and identifies weakly forced environments as those exhibiting a spatial (area) range of 500-hPa wind speeds less than 12 m s^{-1}. This method is herein referred to as the Illinois method, as it was developed by Carleton et al. (2008a) for characterizing the convective environment in and around Lincoln, Illinois. The third automated method is from Brimelow et al. (2011). It identifies weakly forced environments as those in which the area-averaged daily 500-hPa omega, a measure of vertical motion in the atmosphere, is less than or equal to -1 μbar s^{-1}. This method is herein referred to as the Canadian method, as it was used by Brimelow et al. (2011) to investigate land–atmosphere interactions in the Canadian Prairies. Hourly surface wind speed, 500-hPa wind speed, and omega data were taken from the Modern-Era Retrospective Analysis for Research and Applications, version 2 (MERRA-2; Bosilovich et al. 2015). MERRA-2 is produced by the NASA Global Modeling and Assimilation Office using the GEOS-5.12.4 modeling system. The hourly wind and omega datasets are available at a 0.5° × 0.625° spatial resolution from 1980 to the present. The MERRA-2 system assimilates observations from atmospheric in situ and remote sensing sources. Each day between May and September 2005–07 for each individual 5° × 5° region was identified as either weakly or synoptically forced using each of the four classification methods (1 manual + 3 automated).

c. *Soil moisture–precipitation coupling*

Soil moisture anomalies collocated with convection initiation events were composited and evaluated to determine whether there were statistically significant preferences for wet or dry soil coupling. Our evaluation uses two approaches. First, we compared the distribution of soil moisture anomalies at the location of convection initiation with equally sized distributions of soil moisture anomalies from randomly selected locations in the study region. For example, if soil moisture anomalies associated with 8000 thunderstorm events are composited, then 8000 locations randomly chosen from the entire study area were composited. This random sampling process was repeated 1000 times using a bootstrapping resampling procedure (with replacement). This produces a large sample that can be used to evaluate whether the soil

moisture conditions associated with convection initiation were significantly different from what could be expected due to random chance. This procedure is similar to that employed by Ford et al. (2015a), only here the sample size is orders of magnitude larger. Second, we directly compared the distributions of soil moisture conditions associated with the thunderstorm events, grouped by 1) soil moisture dataset, 2) convective environment (weakly or synoptically forced), and 3) the method by which the convective environment is classified. Direct comparison between these various groups was done using a series of two-way analysis of variance (ANOVA) with multiple comparison tests to determine where significant differences exist. The primary purpose of the ANOVA is to determine the extent and significance of differences in soil moisture data and synoptic environment on apparent wet soil or dry soil preferences for soil moisture–precipitation coupling in the Great Plains.

4. Results

a. Convective environment classification

Not surprisingly, the number of afternoon thunderstorm events are not equally distributed among the 12 Great Plains areas (see Table 3 for area abbreviations). The southern quarter of our study region—WTX, RRB, and LOU regions—has much higher frequencies of thunderstorm events. This can be mostly attributed to the abundant supply of convective available potential energy, particularly in the RRB and LOU regions, and the proximity of these areas to the Gulf of Mexico (Lock and Houston 2015). Based on manual identification, these three areas exhibited the highest frequencies of weakly forced days (Fig. 3a), and this pattern is consistent between all five months of the warm season (Fig. 3b). It is important to note that the frequencies and percentages shown in Fig. 3 are for all days classified, not just days with thunderstorm events. The manual classification procedure is considered the benchmark against which the automated methods can be compared. When comparing 1-to-1 the percent of overall days between May and September 2005–07 that are classified as weakly forced, we see similar performance (as verified by the manual method) from the Georgia and Illinois methods (Fig. 4). In general, these methods capture the frequency of weakly forced days in the southern and southeastern regions, but they do not do as well in the northern and northwestern regions. Specifically, both methods underestimate the frequency of weakly forced days in Nebraska, the Dakotas, Minnesota, and Iowa. This is possibly attributable to the fact that these methods—and their synoptic-scale wind speed thresholds—were developed for areas farther south and east than these regions. The Canadian method, in contrast, overestimates the number of weakly forced days relative to the manual classification method. In fact, it classifies over 80% of days in all of the regions as weakly forced. Therefore, the Canadian method appears to suffer from the opposite problem as the Georgia and Illinois methods. Since it was designed for a region with less CAPE and fewer thunderstorm events, it significantly overestimates in all regions.

Of course, it should be noted that none of these methods were developed for a continental-scale analysis. Therefore, it is not unexpected that they do not perform as well in regions that differ from where they were developed. However, even when applied outside of the geographic areas in which they were developed, the Georgia and Illinois methods do correspond well with the manual classification results. This is true for all days in the study period as well as for just days and locations in which afternoon thunderstorm events occurred (Fig. 4). The Illinois method (red circles) and Georgia method (blue circles) are within 10% and 30% of the manual classification method (yellow squares) with respect to the proportion of ThOR events classified as weakly forced. Additionally, the 16 083 ThOR events are plotted in dual convective triggering potential low-level humidity index (CTP-HI; Findell and Eltahir 2003) space, often used to identify atmospheric conditions primed for land surface–induced convective activity (Fig. 4). Specifically, negative CTP values indicate atmospheric conditions not conducive to surface-influenced or surface-triggered convection. The red points in these plots show all afternoon ThOR events, and the blue only show the weakly forced events. The CTP range is reduced for weakly forced events compared with all events, with fewer negative CTP values. This indicates that the boundary layer atmosphere is primed for convection over dry or wet soils and lends confidence that the manual, Georgia, and Illinois methods are properly filtering thunderstorm events that have the potential to be triggered by soil moisture–induced processes.

b. Precipitation persistence

Precipitation/atmospheric persistence refers to consecutive measurements that are not independent of one another. That is, the consecutive events are attributed to the same meteorological system. These incidents can result in elevated lag-1 daily precipitation autocorrelation and possibly inflated inferences of positive soil moisture feedbacks (Wei et al. 2008). Previous studies have attempted to account for precipitation persistence

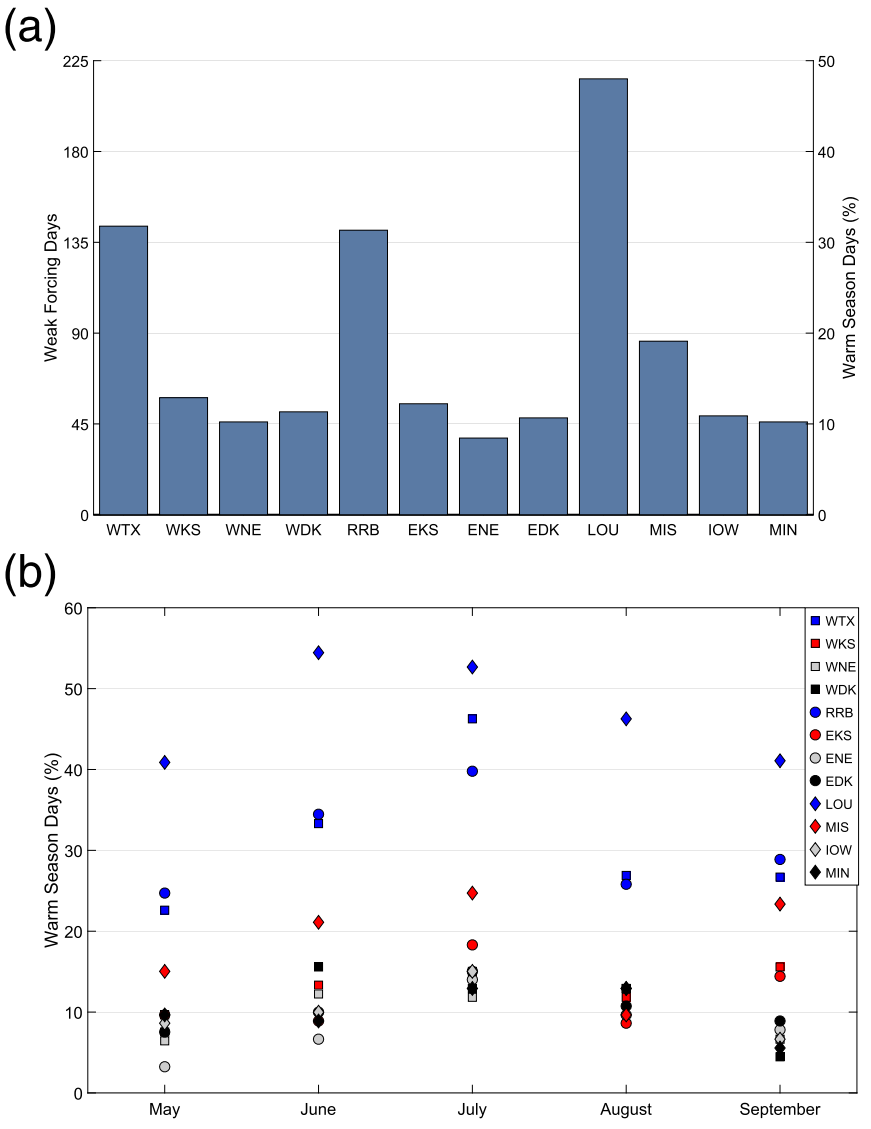

FIG. 3. (a) Total number of weakly forced days in each region based on the manual classification method. (b) Percent of warm season days in each calendar month that are classified as weakly forced days, based on the manual classification. All days between May and September 2005–07 are classified.

in a general way (Taylor et al. 2012; Guillod et al. 2014; Ford et al. 2015b) and, in a few cases, using a methodology explicitly designed to control for this effect (Salvucci et al. 2002; Tuttle and Salvucci 2016). The more sophisticated methods have effectively isolated a statistical feedback signal; however, this signal may also not represent the true soil moisture feedback if the filtering process they employed removed part of the soil moisture feedback signal. For example, the lag-1 daily precipitation autocorrelation at any particular point in the Great Plains (Fig. 5) is influenced by precipitation persistence due to large-scale synoptic weather systems that induce precipitation on consecutive days, but it is also potentially influenced by positive or negative soil moisture feedback. The May–September lag-1 precipitation autocorrelation (Fig. 5) is computed from daily data that are part of the Parameter-Elevation Regressions on Independent Slopes Model (PRISM) using Wilks (1999) method, such that

$$r = p_{11} - p_{01},$$

where r is the lag-1 autocorrelation coefficient, p_{11} is the transition probability of precipitation on day n given precipitation on day $n - 1$, and p_{01} is the transition

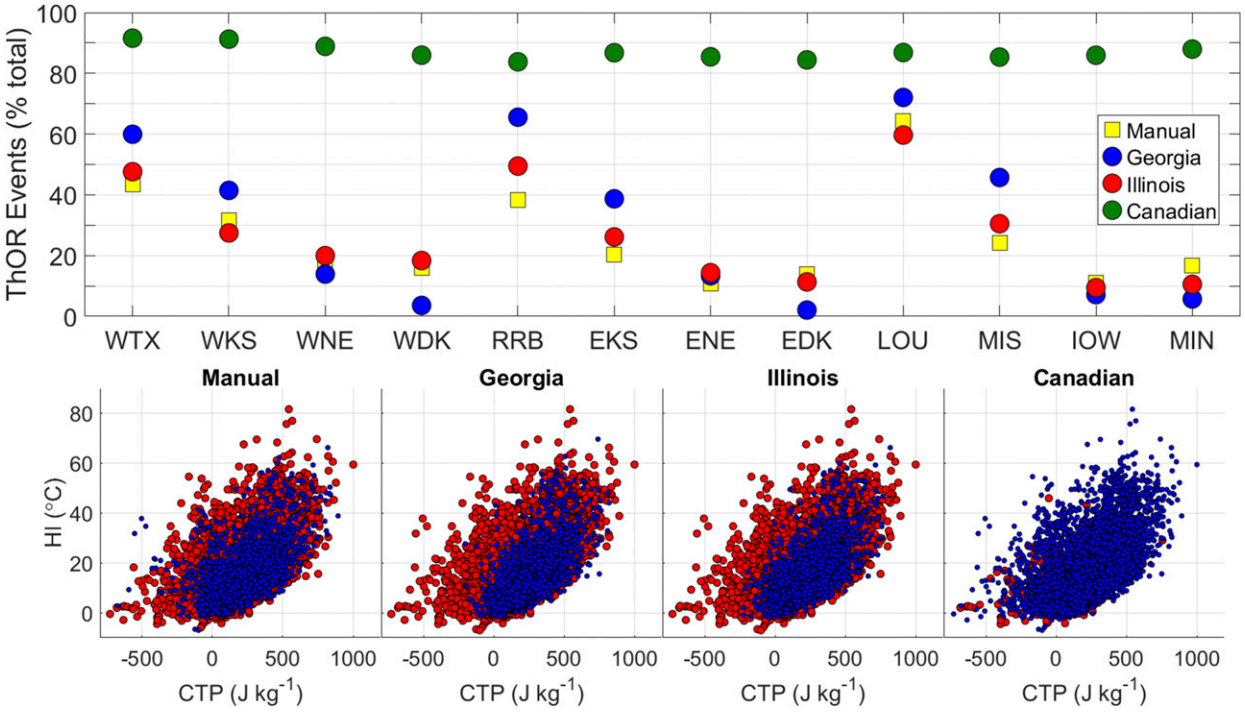

FIG. 4. (top) The percentage of ThOR afternoon thunderstorm events classified as weakly forced by each of the four classification methods. (bottom) All ThOR afternoon thunderstorm events plotted in dual CTP-HI space, computed from MERRA-2. Red points show all events; blue points show weakly forced events.

probability of precipitation on day n given no precipitation on day $n - 1$.

By classifying each thunderstorm event as either synoptically forced or weakly forced, we can account for the inherent precipitation persistence in the lag-1 autocorrelations. We classify each ThOR event based on 1) whether it was synoptically or weakly forced, 2) whether or not rain occurred in a 5×5 (PRISM) grid cell area surrounding the initiation point the day before, and 3) whether any precipitation the day before was synoptically or weakly forced. The result of this classification is a set of six possible outcomes for any thunderstorm event that occurs on day n and the preceding day $n - 1$: synoptic to synoptic, weak to synoptic, synoptic to weak, weak to weak, none to synoptic, and none to weak. For clarification, the synoptic-to-synoptic outcome indicates that synoptically forced precipitation originated both on day n and on day $n - 1$, whereas the synoptic-to-weak outcome indicated that synoptically forced precipitation originated on day $n - 1$, but the thunderstorm event on day n was weakly forced. Of these six outcomes, only the synoptic-to-synoptic and weak-to-synoptic classes contribute to precipitation persistence, and these outcomes together make up less than 50% of thunderstorm events in all regions (Fig. 6). In fact, fewer than 40% of thunderstorm events in the Red River basin region contributed to precipitation persistence, despite this region exhibiting the strongest overall lag-1 precipitation autocorrelation (Fig. 5). The synoptic-to-weak, weak-to-weak, and none-to-weak outcomes can potentially indicate a soil moisture feedback and only comprise a small fraction of all thunderstorm events (Fig. 6). The none-to-synoptic outcome is a confounding factor that is not accounted for when considering precipitation persistence. These events are triggered by a synoptic-scale forcing, and therefore land surface conditions have minimal influence. However, if the forcing classification (weak versus strong) is not used, these events that make up the majority of two-thirds of the regions' thunderstorms (Fig. 6) will be inadvertently included in the soil moisture–precipitation feedback assessment. This means that in most of the regions assessed, the importance—in terms of the proportion of all thunderstorm events—of accounting for the convective forcing outweighed that of precipitation persistence; however, both are confounding factors that soil moisture–precipitation feedback studies should recognize and account for using appropriate methods.

c. *Wet and dry soil preferences*

To determine whether there are preferences for thunderstorms to initiate over relatively wet or relatively dry

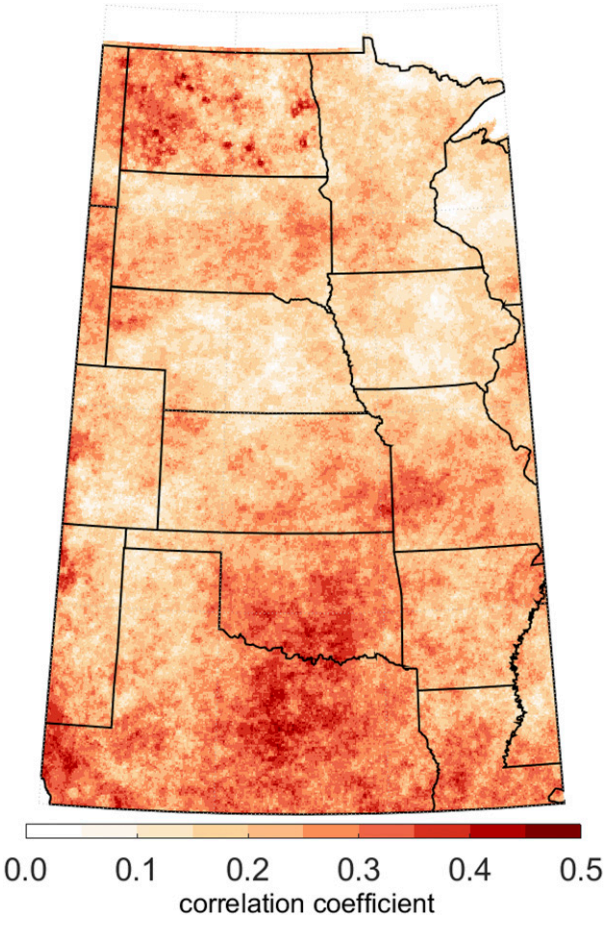

FIG. 5. Lag-1 daily precipitation autocorrelation calculated according to Wilks (1999). Daily precipitation is between May and September 2005–07 using the PRISM dataset.

soils (delineated by a soil moisture anomaly of 0), we composited soil moisture anomalies from all three remote sensing products collocated with the 16 083 ThOR events. We then randomly sampled the same number of soil moisture anomalies in both space (all regions) and in time (all study days, May–September 2005–07) and composited soil moisture from each of the three products underlying these randomly selected points. Additionally, we randomly sampled the same number of soil moisture anomalies in space only, across all regions but on the same days as ThOR thunderstorm events. The resampling was repeated 1000 times using a bootstrapping resampling method with replacement. This resulted in 1000 distributions of 16 083 resampled, time–space soil moisture anomalies and 1000 distributions of 16 083 resampled, space-only soil moisture anomalies, from which a distribution could be constructed and compared with the distribution of soil moisture anomalies underlying ThOR events. This comparison is facilitated by plotting each of the 1000 bootstrapped composites as well as the thunderstorm event soil moisture in mean standard deviation space (Fig. 7). The blue points in Fig. 7 represent the mean and standard deviation of the soil moisture anomaly distributions randomly sampled in space and time, while the red points represent the mean and standard deviation of the soil moisture anomaly distributions randomly sampled in space only. Statistically significant differences are determined using a difference of means test with a confidence threshold of 95%.

Our results show that when AMSR-E is used to characterize soil moisture conditions, the 16 083 afternoon thunderstorm events tend to occur over drier soils (Fig. 7). ECV and TMI, on the other hand, show a statistically significant preference for convection initiation to occur over wet soils (Fig. 7), although the absolute differences in means are less than those for AMSR-E.

When we only examine the weakly forced thunderstorm events (based on the manual classification method), the results show the same general patterns and preferences as those based on all thunderstorm events. AMSR-E has a dry soil preference and ECV and TMI have wet soil preferences (Fig. 7), all of which are statistically significant. Substituting the Georgia and Illinois classification methods for the manual method of identifying weakly and synoptically forced events does not result in a statistically significant change in the dry/wet soil preferences (results not shown).

Our results demonstrate that apparent preferences for convection initiation in the Great Plains occur over relatively wet or dry soils, and the statistical significance of these preferences is sensitive to the soil moisture dataset, the convective forcing, and the method by which the convective forcing is classified. The distinct and interactive effects of these confounding factors are examined more thoroughly through a series of two-way ANOVA tests with an interaction effect included. The ANOVA examines differences in soil moisture anomalies grouped by dataset and by convective forcing (weak or synoptic). Statistically significant (95% confidence level) differences exist between soil moisture anomalies grouped by dataset, but not by convective forcing (Table 4); however, the interaction term is significant. This occurs because differences in soil moisture anomalies between weakly forced events and all events are statistically significant for AMSR-E, but not for ECV or TMI (Fig. 8), meaning that discriminating between weakly forced and synoptically forced events significantly affects the overall dry/wet soil preference, but only depending on the dataset.

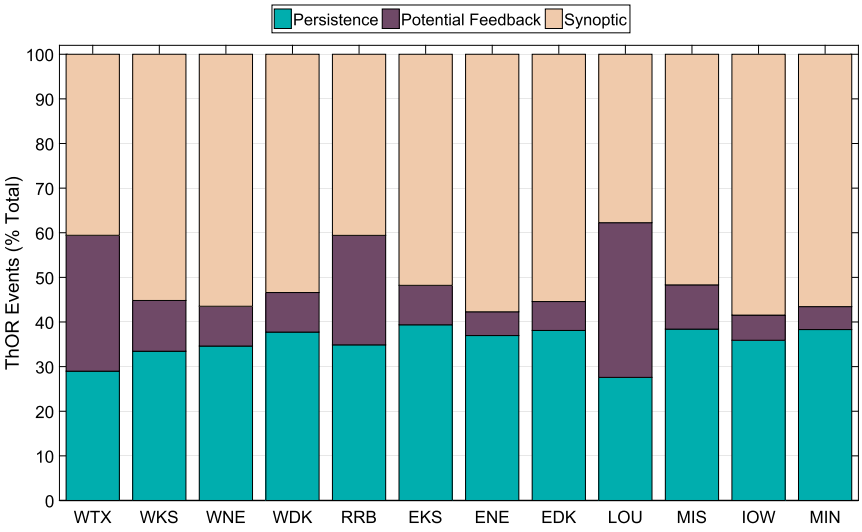

FIG. 6. Percentage of all convection initiation events that are associated with the following categories: 1) ''persistence'' events are those that are synoptically forced and that occur on the day after a weakly or synoptically forced event, 2) ''potential feedback'' events are those that are weakly forced irrespective of what occurred the day before, and 3) ''synoptic'' events are those that are synoptically forced and follow a day in which no precipitation occurred.

A second ANOVA is used to examine differences in soil moisture preferences grouped both by dataset and by the convective forcing classification method (i.e., manual, Georgia, and Illinois). In this case, days being compared are classified as ''weakly forced'' by one of the classification methods. Statistically significant differences exist both between soil moisture based on the dataset and classification method (Table 4). Additionally, the interaction term is significant, again a result of there being a significant soil moisture anomaly difference between manually classified events and those classified based on the Illinois method, but only for AMSR-E (Fig. 8). Practically, all three classification methods show significant AMSR-E dry soil preferences for weakly forced afternoon convection initiation.

5. Discussion and conclusions

The recommendations provided by Tuttle and Salvucci (2017) with respect to how to undertake a statistical analysis of soil moisture–precipitation feedbacks, including those related to soil moisture time-scale variability and precipitation persistence, are important to consider. The seasonality of soil moisture in many global transition regions is well documented (e.g., Illston et al. 2008) and must be accounted for to properly characterize relative soil wetness. Additionally, our results show that the precision with which soil moisture estimates are reported dictates the methods that can be applied to standardize or remove the seasonal cycle of soil moisture datasets. Although converting volumetric water content to percentiles both standardizes and deseasonalizes soil moisture data, this method is not recommended when measurement precision is limited. For example, AMSR-E and TMI datasets are reported in 1% volumetric water content increments and therefore cannot be properly converted to percentiles.

Precipitation/atmospheric persistence is often identified as a serious confounding issue when analyzing soil moisture–precipitation feedbacks using observations (Taylor et al. 2011; Guillod et al. 2015; Tuttle and Salvucci 2016; Hsu et al. 2017) because it can inflate or deflate potential soil moisture feedback signals (Wei et al. 2008; Tuttle and Salvucci 2017). We find that the lag-1 autocorrelation of daily precipitation is only partially attributable to precipitation persistence, defined here as a situation in which a synoptically forced afternoon thunderstorm event follows an event (weakly or synoptically forced) in the same location occurring the day prior. In fact, these situations account for less than 50% of all afternoon thunderstorm events identified over the 2005–07 study period in all regions of the Great Plains. Far more common were synoptically forced thunderstorm events that were preceded by days without precipitation. Despite not contributing to precipitation persistence, these events equally confound statistical analysis of soil moisture–precipitation

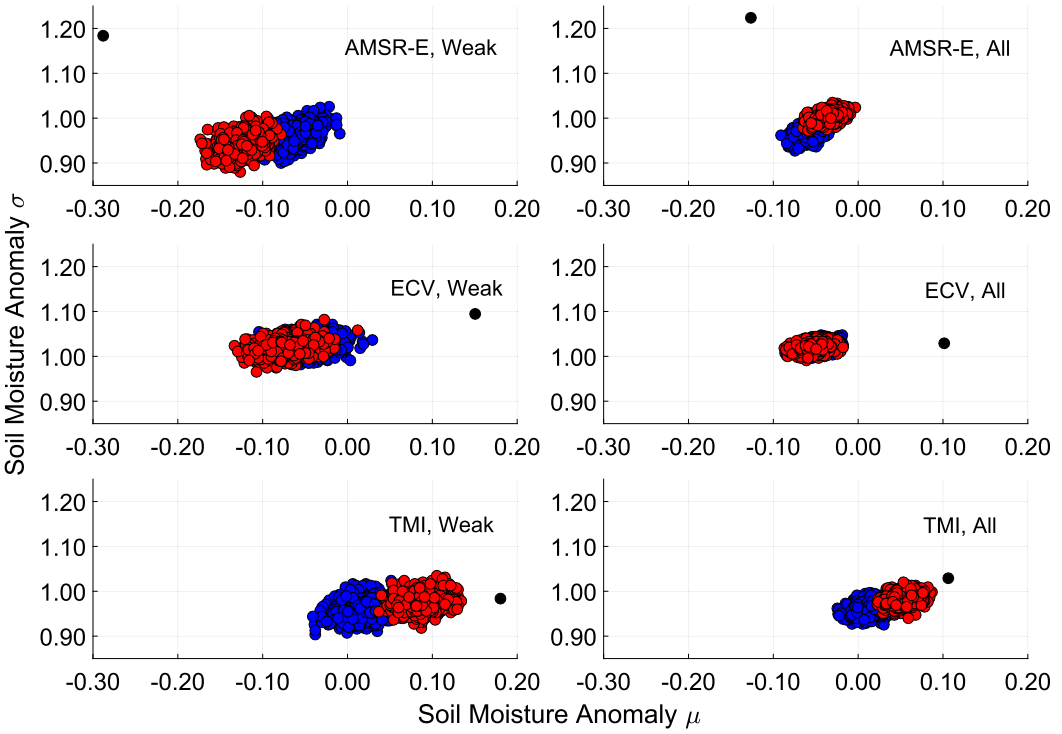

FIG. 7. Panels show the mean and standard deviation of soil moisture anomalies underlying afternoon thunderstorm events (black point), those from distributions of randomly selected points in space (red points), and those from distributions of randomly selected points in space and time (blue). Soil moisture anomalies are from (top) AMSR-E, (middle) ECV, and (bottom) TMI for (left) just weakly forced events and (right) all afternoon events

feedback as convection is not primarily attributed to land surface conditions. Our methodology that combines ThOR-identified afternoon thunderstorm events with a classification of the overall convective environment not only accounts for precipitation persistence, it also effectively isolates the events where the land surface can potentially play a role in triggering convection. An added advantage of using ThOR is the ability to identify the location of convection initiation. This eliminates the reliance on precipitation datasets and provides a more accurate means of associating soil moisture conditions with the location where convection occurred.

It is interesting to note that removing the effects of precipitation persistence and synoptic-scale forcing did not result in a change in the sign of the preference for deep convection to initiate over dry or wet soils. However, the use of three X-band microwave remote sensing soil moisture datasets did expose significant interdataset differences in both the strength and sign of dry/wet soil preferences. Composites of AMSR-E soil moisture underlying afternoon thunderstorm events exhibit a statistically significant dry soil preference, while the same composites of ECV and TMI soil moisture exhibit significant wet soil preferences. This is the case despite the fact that AMSR-E is the primary passive microwave imager informing the ECV dataset during the 2005–07 time period studied (Dorigo et al. 2015). In addition to differences in soil moisture dataset and convective forcing, we tested three automated methods for classifying weakly forced events. Although

TABLE 4. Two-way ANOVA tables with interactions to assess whether there are significant differences in soil moisture anomalies. The top part of the table shows results testing differences in all ThOR event–soil moisture anomalies grouped by dataset and convective forcing. The bottom part of the table shows results testing differences in weakly forced ThOR event–soil moisture anomalies grouped by dataset and convective environment classification method.

Source	F stat	p value
All events		
Dataset	297.84	0.00
Forcing	0.10	0.75
Dataset-forcing interaction	23.80	0.00
Weakly forced events		
Dataset	861.35	0.00
Classification method	6.96	0.00
Interactions	4.29	0.00

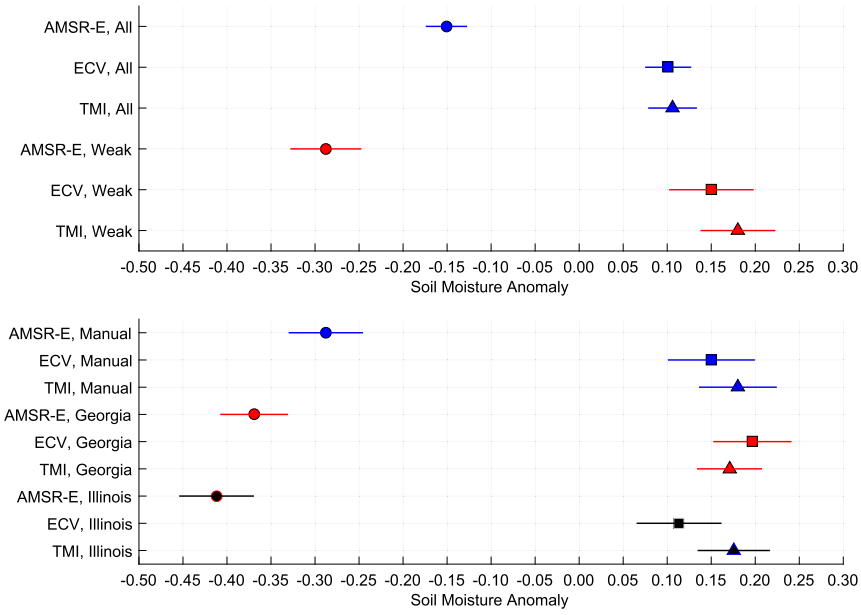

FIG. 8. Distributions of soil moisture anomalies grouped by (top) dataset and convective forcing (weak = weakly forced) and (bottom) dataset and classification method. Significant differences between distributions exist at the 95% confidence level if the lines do not overlap.

differences existed between these automated methods and our manual classification, these differences did not result in significant changes in the sign of dry/wet soil preferences.

Our results concur with those of Tuttle and Salvucci (2017), and we conclude that observational analyses of soil moisture–precipitation feedbacks must be completed with care. However, we find that accounting for precipitation persistence, although necessary and important, did not influence our results with regard to dry/wet soil preferences. In addition, the different remote sensing datasets had a larger impact on the analysis than precipitation persistence. It is unclear whether the results of our sensitivity analysis are universal, or whether the results would differ in other parts of the world due to spatial variations in the accuracy of the satellite retrievals and variations in the importance of precipitation persistence. In addition, it is important to note here that the objective of this study was not to determine whether there is a preference for convection initiation to occur preferentially over wet or dry soils in the U.S. Great Plains, but instead to demonstrate how dependent these apparent preferences are to certain confounding factors and the datasets and methods that are used. Based on the results presented here, we recommend that future studies of soil moisture–precipitation feedbacks should 1) consider and account for the convective environment (weakly or synoptically forced) and 2) use multiple soil moisture and/or precipitation datasets to determine whether the whether the soil moisture feedback is robust.

Acknowledgments. This work was supported by NASA Grant NNX16AO97G.

REFERENCES

Albergel, C., P. de Rosnay, C. Gruhier, J. Muñoz-Sabater, S. Hasenauer, L. Isaksen, Y. Kerr, and W. Wagner, 2012: Evaluation of remotely sensed and modelled soil moisture products using global ground-based in situ observations. *Remote Sens. Environ.*, **118**, 215–226, https://doi.org/10.1016/j.rse.2011.11.017.

Alfieri, L., P. Claps, P. D'Odorico, F. Laio, and T. M. Over, 2008: An analysis of the soil moisture feedback on convective and stratiform precipitation. *J. Hydrometeor.*, **9**, 280–291, https://doi.org/10.1175/2007JHM863.1.

Bindlish, R., T. J. Jackson, E. Wood, H. Gao, P. Starks, D. Bosch, and V. Lakshmi, 2003: Soil moisture estimates from TRMM Microwave Imager observations over the southern United States. *Remote Sens. Environ.*, **85**, 507–515, https://doi.org/10.1016/S0034-4257(03)00052-X.

Bosilovich, M. G., and Coauthors, 2015: MERRA-2: Initial evaluation of the climate. NASA Tech. Memo. NASA/TM-2015-104606/Vol. 43, 145 pp., https://gmao.gsfc.nasa.gov/pubs/docs/Bosilovich803.pdf.

Brimelow, J. C., J. M. Hanesiak, and W. R. Burrows, 2011: Impacts of land–atmosphere feedbacks on deep, moist convection on the Canadian Prairies. *Earth Interact.*, **15**, https://doi.org/10.1175/2011EI407.1.

Brown, M. E., and D. L. Arnold, 1998: Land-surface–atmosphere interactions associated with deep convection in Illinois. *Int. J. Climatol.*, **18**, 1637–1653, https://doi.org/10.1002/(SICI)1097-0088(199812)18:15<1637::AID-JOC336>3.0.CO;2-U.

Carleton, A. M., D. L. Arnold, D. J. Travis, S. Curran, and J. O. Adegoke, 2008a: Synoptic circulation and land surface influences on convection in the Midwest U.S. "corn belt" during the summers of 1999 and 2000. Part I: Composite synoptic

environments. *J. Climate*, **21**, 3389–3415, https://doi.org/10.1175/2007JCLI1578.1.

——, D. J. Travis, J. O. Adegoke, D. L. Arnold, and S. Curran, 2008b: Synoptic circulation and land surface influences on convection in the Midwest US "corn belt" during the summers of 1999 and 2000. Part II: Role of vegetation boundaries. *J. Climate*, **21**, 3617–3641, https://doi.org/10.1175/2007JCLI1584.1.

Dirmeyer, P. A., and Coauthors, 2016: Confronting weather and climate models with observational data from soil moisture networks over the United States. *J. Hydrometeor.*, **17**, 1049–1067, https://doi.org/10.1175/JHM-D-15-0196.1.

Dixon, P. G., and T. L. Mote, 2003: Patterns and causes of Atlanta's urban heat island–initiated precipitation. *J. Appl. Meteor.*, **42**, 1273–1284, https://doi.org/10.1175/1520-0450(2003)042<1273:PACOAU>2.0.CO;2.

Dorigo, W. A., and Coauthors, 2015: Evaluation of the ESA CCI soil moisture product using ground-based observations. *Remote Sens. Environ.*, **162**, 380–395, https://doi.org/10.1016/j.rse.2014.07.023.

——, and Coauthors, 2017: ESA CCI soil moisture for improved Earth system understanding: State-of-the-art and future directions. *Remote Sens. Environ.*, **203**, 185–215, https://doi.org/10.1016/j.rse.2017.07.001.

Eltahir, E. A. B., 1998: A soil moisture-rainfall feedback mechanism: 1. Theory and observations. *Water Resour. Res.*, **34**, 765–776, https://doi.org/10.1029/97WR03499.

Evans, J. S., and C. A. Doswell III, 2001: Examination of derecho environments using proximity soundings. *Wea. Forecasting*, **16**, 329–342, https://doi.org/10.1175/1520-0434(2001)016<0329:EODEUP>2.0.CO;2.

Ferguson, C. R., and E. F. Wood, 2011: Observed land–atmosphere coupling from satellite remote sensing and reanalysis. *J. Hydrometeor.*, **12**, 1221–1254, https://doi.org/10.1175/2011JHM1380.1.

Findell, K. L., and E. A. B. Eltahir, 2003: Atmospheric controls on soil moisture–boundary layer interactions. Part I: Framework development. *J. Hydrometeor.*, **4**, 552–569, https://doi.org/10.1175/1525-7541(2003)004<0552:ACOSML>2.0.CO;2.

——, P. Gentine, B. R. Lintner, and C. Kerr, 2011: Probability of afternoon precipitation in eastern United States and Mexico enhanced by high evaporation. *Nat. Geosci.*, **4**, 434–439, https://doi.org/10.1038/ngeo1174.

Ford, T. W., A. D. Rapp, and S. M. Quiring, 2015a: Does afternoon precipitation occur preferentially over dry or wet soils in Oklahoma? *J. Hydrometeor.*, **16**, 874–888, https://doi.org/10.1175/JHM-D-14-0005.1.

——, ——, ——, and J. Blake, 2015b: Soil moisture–precipitation coupling: Observations from the Oklahoma Mesonet and underlying physical mechanisms. *Hydrol. Earth Syst. Sci.*, **19**, 3617–3631, https://doi.org/10.5194/hess-19-3617-2015.

——, Q. Wang, and S. M. Quiring, 2016: The observation record length necessary to generate robust soil moisture percentiles. *J. Appl. Met. Climatol.*, **55**, 2131–2149, https://doi.org/10.1175/JAMC-D-16-0143.1.

French, A. J., and M. D. Parker, 2012: Observations of mergers between squall lines and isolated supercell thunderstorms. *Wea. Forecasting*, **27**, 255–278, https://doi.org/10.1175/WAF-D-11-00058.1.

Frye, J. D., and T. L. Mote, 2010: Convection initiation along soil moisture boundaries in the southern Great Plains. *Mon. Wea. Rev.*, **138**, 1140–1151, https://doi.org/10.1175/2009MWR2865.1.

Gao, H., E. F. Wood, T. J. Jackson, M. Drusch, and R. Bindlish, 2006: Using TRMM/TMI to retrieve surface soil moisture over the southern United States from 1998 to 2002. *J. Hydrometeor.*, **7**, 23–38, https://doi.org/10.1175/JHM473.1.

Guillod, B. P., and Coauthors, 2014: Land-surface controls on afternoon precipitation diagnosed from observational data: Uncertainties and confounding factors. *Atmos. Chem. Phys.*, **14**, 8343–8367, https://doi.org/10.5194/acp-14-8343-2014.

——, B. Orlowsky, D. G. Miralles, A. J. Teuling, and S. I. Seneviratne, 2015: Reconciling spatial and temporal soil moisture effects on afternoon rainfall. *Nat. Commun.*, **6**, 6443, https://doi.org/10.1038/ncomms7443.

Hirschi, M., B. Mueller, W. Dorigo, and S. I. Seneviratne, 2014: Using remotely sensed soil moisture for land–atmosphere coupling diagnostics: The role of surface vs. root-zone soil moisture variability. *Remote Sens. Environ.*, **154**, 246–252, https://doi.org/10.1016/j.rse.2014.08.030.

Houston, A. L., N. A. Lock, J. Lahowetz, B. L. Barjenbruch, G. Limpert, and C. Oppermann, 2015: Thunderstorm Observation by Radar (ThOR): An algorithm to develop a climatology of thunderstorms. *J. Atmos. Oceanic Technol.*, **32**, 961–981, https://doi.org/10.1175/JTECH-D-14-00118.1.

Hsu, H., M.-H. Lo, B. P. Guillod, D. G. Miralles, and S. Kumar, 2017: Relation between precipitation location and antecedent/subsequent soil moisture spatial patterns. *J. Geophys. Res. Atmos.*, **122**, 6319–6328, https://doi.org/10.1002/2016JD026042.

Hu, X., M. Xue, and R. A. McPherson, 2017: The importance of soil-type contrast in modulating August precipitation distribution new the Edwards Plateau and Balcones Escarpment in Texas. *J. Geophys. Res. Atmos.*, **122**, 10 711–10 728, https://doi.org/10.1002/2017JD027035.

Illston, B. G., J. B. Basara, C. A. Fiebrich, K. C. Crawford, E. Hunt, D. K. Fisher, R. Elliott, and K. Humes, 2008: Mesoscale monitoring of soil moisture across a statewide network. *J. Atmos. Oceanic Technol.*, **25**, 167–182, https://doi.org/10.1175/2007JTECHA993.1.

Khong, A., J. K. Wang, S. M. Quiring, and T. W. Ford, 2015: Soil moisture variability in Iowa. *Int. J. Climatol.*, **35**, 2837–2848, https://doi.org/10.1002/joc.4176.

Koster, R. D., and Coauthors, 2004: Regions of strong coupling between soil moisture and precipitation. *Science*, **305**, 1138–1140, https://doi.org/10.1126/science.1100217.

Kummerow, C., W. Barnes, T. Kozu, J. Shiue, and J. Simpson, 1998: The Tropical Rainfall Measuring Mission (TRMM) sensor package. *J. Atmos. Oceanic Technol.*, **15**, 809–817, https://doi.org/10.1175/1520-0426(1998)015<0809:TTRMMT>2.0.CO;2.

Legates, D. R. R., R. Mahmood, D. F. Levia, T. L. DeLiberty, S. M. Quiring, C. Houser, and F. E. Nelson, 2011: Soil moisture: A central and unifying theme in physical geography. *Prog. Phys. Geogr.*, **35**, 65–86, https://doi.org/10.1177/0309133310386514.

Liu, Y. Y., W. A. Dorigo, R. M. Parinussa, R. A. M. de Jeu, W. Wagner, M. F. McCabe, J. P. Evans, and A. I. J. M. van Dijk, 2012: Trend-preserving blending of passive and active microwave soil moisture retrievals. *Remote Sens. Environ.*, **123**, 280–297, https://doi.org/10.1016/j.rse.2012.03.014.

Lock, N. A., and A. L. Houston, 2014: Empirical examination of the factors regulating thunderstorm initiation. *Mon. Wea. Rev.*, **142**, 240–258, https://doi.org/10.1175/MWR-D-13-00082.1.

——, and ——, 2015: Spatiotemporal distribution of thunderstorm initiation in the US Great Plains from 2005 to 2007. *Int. J. Climatol.*, **35**, 4047–4056, https://doi.org/10.1002/joc.4261.

McPherson, R. A., 2007: A review of vegetation—Atmosphere interactions and their influences on mesoscale phenomena. *Prog. Phys. Geogr.*, **31**, 261–285, https://doi.org/10.1177/0309133307079055.

Miralles, D. G., M. J. van den Berg, A. J. Teuling, and R. A. M. de Jeu, 2012: Soil moisture-temperature coupling: A multiscale observational analysis. *Geophys. Res. Lett.*, **39**, L21707, https://doi.org/10.1029/2012GL053703.

Njoku, E. G., T. J. Jackson, V. Lakshmi, T. K. Chang, and S. V. Nghiem, 2003: Soil moisture retrieval from AMSR-E. *IEEE Trans. Geosci. Remote Sens.*, **41**, 215–229, https://doi.org/10.1109/TGRS.2002.808243.

Owe, M., R. de Jeu, and T. Holmes, 2008: Multisensor historical climatology of satellite-derived global land surface moisture. *J. Geophys. Res.*, **113**, F01002, https://doi.org/10.1029/2007JF000769.

Pal, J. S., and E. A. B. Eltahir, 2001: Pathways relating soil moisture conditions to future summer rainfall within a model of the land–atmosphere system. *J. Climate*, **14**, 1227–1242, https://doi.org/10.1175/1520-0442(2001)014<1227:PRSMCT>2.0.CO;2.

Rose, L. S., J. A. Stallins, and M. L. Bentley, 2008: Concurrent cloud-to-ground lightning and precipitation enhancement in the Atlanta, Georgia (United States), urban region. *Earth Interact.*, **12**, https://doi.org/10.1175/2008EI265.1.

Salvucci, G. D., J. A. Saleem, and R. Kaufmann, 2002: Investigating soil moisture feedbacks on precipitation with tests of Granger causality. *Adv. Water Resour.*, **25**, 1305–1312, https://doi.org/10.1016/S0309-1708(02)00057-X.

Santanello, J. A., Jr., C. D. Peters-Lidard, and S. V. Kumar, 2011: Diagnosing the sensitivity of local land–atmosphere coupling via the soil moisture–boundary layer interaction. *J. Hydrometeor.*, **12**, 766–786, https://doi.org/10.1175/JHM-D-10-05014.1.

Scott, B. L., T. E. Ochsner, B. G. Illston, C. A. Fiebrich, J. B. Basara, and A. J. Sutherland, 2013: New soil property database improves Oklahoma Mesonet soil moisture estimates. *J. Atmos. Oceanic Technol.*, **30**, 2585–2595, https://doi.org/10.1175/JTECH-D-13-00084.1.

Su, C., D. Ryu, R. I. Young, A. W. Western, and W. Wagner, 2013: Inter-comparison of microwave satellite soil moisture retrievals over the Murrumbidgee Basin, southeast Australia. *Remote Sens. Environ.*, **134**, 1–11, https://doi.org/10.1016/j.rse.2013.02.016.

Taylor, C. M., A. Gounou, F. Guichard, P. P. Harris, R. J. Ellis, F. Couvreux, and M. De Kauwe, 2011: Frequency of Sahelian storm initiation enhanced over mesoscale soil-moisture patterns. *Nat. Geosci.*, **4**, 430–433, https://doi.org/10.1038/ngeo1173.

——, R. A. M. de Jeu, F. Guichard, P. P. Harris, and W. A. Dorigo, 2012: Afternoon rain more likely over drier soils. *Nature*, **489**, 423–426, https://doi.org/10.1038/nature11377.

Tuttle, S. E., and G. D. Salvucci, 2014: A new approach for validating satellite estimates of soil moisture using large-scale precipitation: Comparing AMSR-E products. *Remote Sens. Environ.*, **142**, 207–222, https://doi.org/10.1016/j.rse.2013.12.002.

——, and ——, 2016: Empirical evidence of contrasting soil moisture–precipitation feedbacks across the United States. *Science*, **352**, 825–828, https://doi.org/10.1126/science.aaa7185.

——, and ——, 2017: Confounding factors in determining causal soil moisture–precipitation feedback. *Water Resour. Res.*, **53**, 5531–5544, https://doi.org/10.1002/2016WR019869.

Wei, J., R. E. Dickinson, and H. Chen, 2008: A negative soil moisture–precipitation relationship and its causes. *J. Hydrometeor.*, **9**, 1364–1376, https://doi.org/10.1175/2008JHM955.1.

Wilks, D. S., 1999: Multisite downscaling of daily precipitation with a stochastic weather generator. *Climate Res.*, **11**, 125–136, https://doi.org/10.3354/cr011125.

Zhou, J., J. Wen, X. Wang, J. Dongyu, and J. Chen, 2016: Analysis of the Qinghai-Xizang Plateau monsoon evolution and its linkages with soil moisture. *Remote Sens.*, **8**, 493, https://doi.org/10.3390/rs8060493.